# Overview of NASA XMS Reference Design

**Prepared by**

**The GSFC/NIST XMS Collaboration**

**Version 2.0**

**7/21/2009**

MICROCALORIMETER ARRAY: The US reference design for the XMS focal plane consists of a composite array of close-packed x-ray calorimeters. Mo/Au transition-edge sensor (TES) thermometers with Bi/Au thermalizing x-ray absorbers are presumed, based on successful demonstrations in smaller arrays. A 40 x 40 central array, arranged on a 0.3 mm (3 arc sec) pitch, is contained within a 52 x 52 array of 0.6 mm pixels. In the outer array, 4 pixels are read by a single TES, and discrimination between the four positions is achieved via pulse-shape analysis. The outer array contains 576 TES thermometers, compared to the 1600 of the inner array. The inner array will achieve a resolution of 2.5 eV at 6 keV and below, with a time constant shorter than 0.3 ms. The requirements imposed on the outer array are relaxed; its pixels will achieve 10 eV resolution with fall times < 2 ms. Figure 1 shows a schematic of the focal plane layout. Figures 2 and 3 contain images of prototype devices for both the inner and outer array concept, along the approach being developed at Goddard.

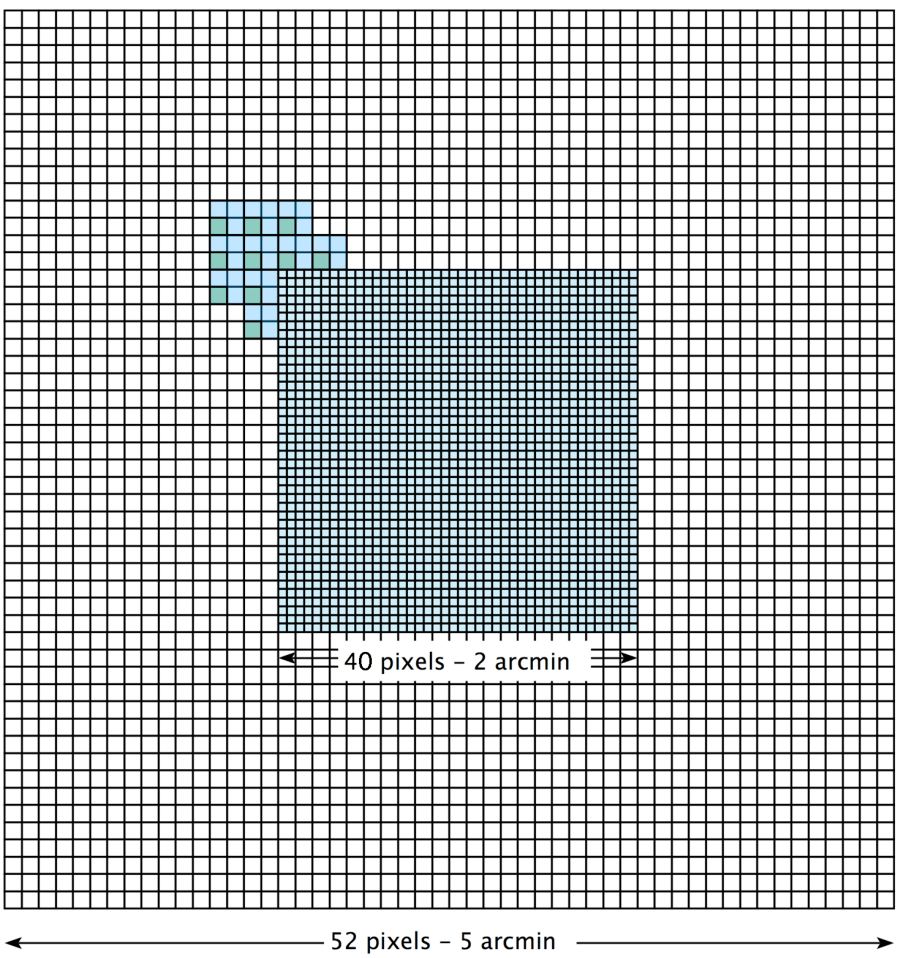


Fig. 1: Schematic of composite calorimeter array at the XMS focal plane. The inner array covers 2 arc min and consists of 3 arc sec pixels with one absorber per TES. The full array covers 5 arc min by use of 6-arcsec outer pixels which are read out by one TES per four absorbers (shown in one corner by marking groups of 4 pixels, each with one TES indicated in green).

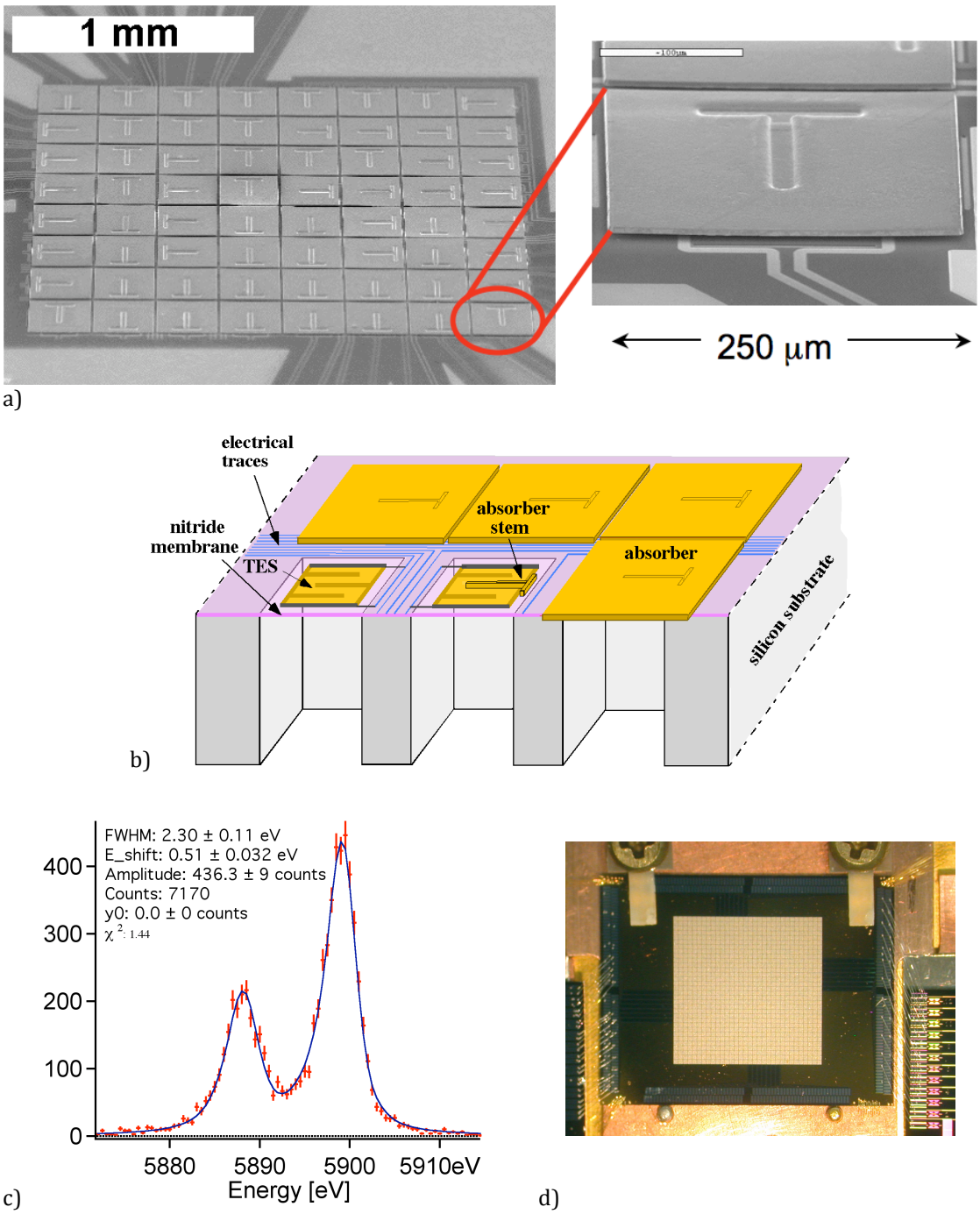


Fig 2: a) Electron micrograph of a Goddard uniform TES array with Au absorbers. The close-up view on the right shows an individual pixel. The absorber is cantilevered over the underlying substrate everywhere except in the T-shaped contact area. b) Schematic showing the structure of a TES array made in the Goddard style. c) Typical resolution of an individual pixel in uniform 8x8 array with Au/Bi absorbers. d) 32x32 array with Au/Bi absorbers.

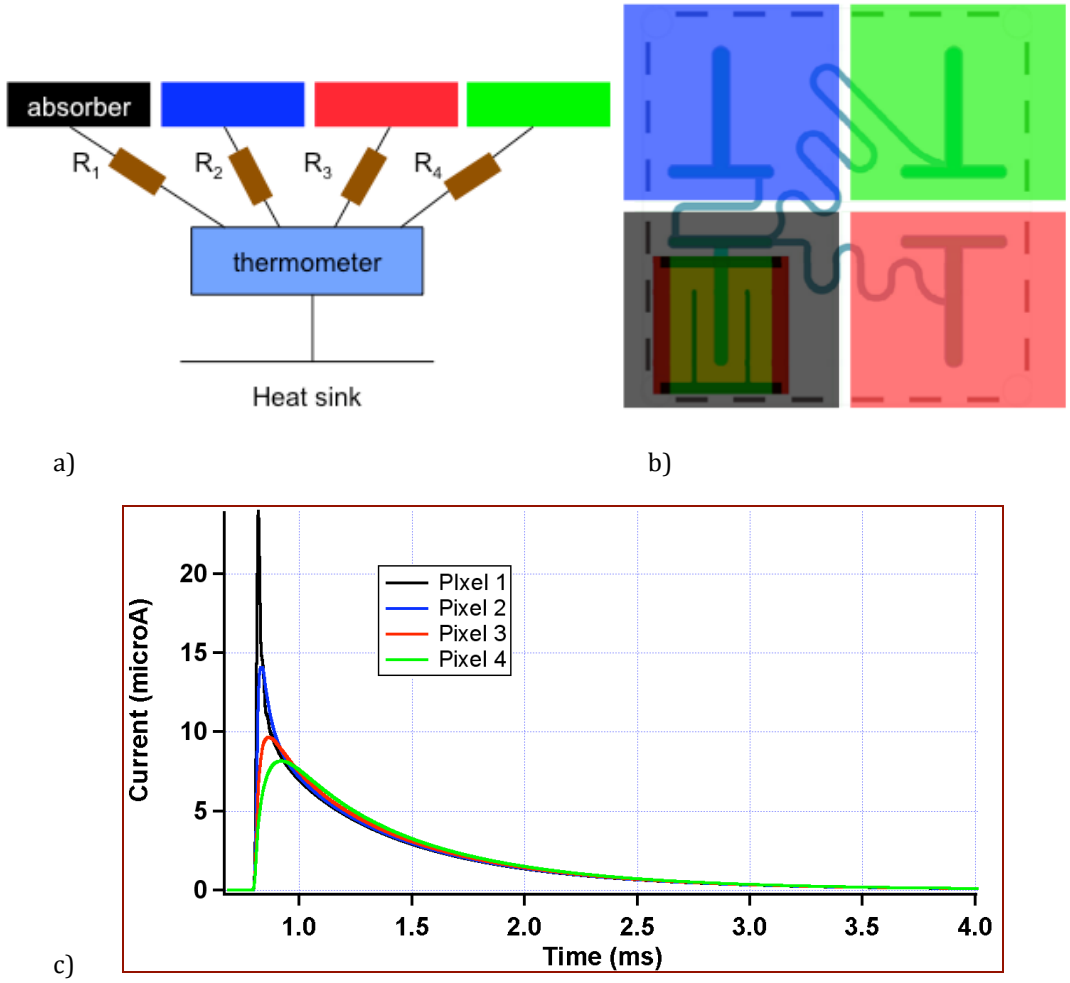


Fig. 3: Ilustrations of the multi-absorber TES concept: a) Four absorbers, shown in different colors, connected to a single TES via different thermal resistances. b) The same as (a), but in a realistic layout. The absorbers are rendered transparent to show the metal meanders that make the different thermal links. The TES is directly under the lower left absorber. c) The corresponding pulse shapes, showing how position is determined by pulse-shape analysis.

MULTIPLEXED SQUID READOUT: Superconducting quantum interference devices (SQUIDs) are well matched to reading the current signals from these low-resistance (typically a few mΩ under optimal bias) sensors. Multiplexed readout is motivated by the need to reduce the number of wires running to the low temperature stages of the instrument for effective management of heat loads and design complexity. In the baseline time-division multiplexing (TDM) concept, the outputs from the dedicated input SQUIDs of individual TES pixels are coupled to a single amplifier, and multiplexing is achieved by sequential switching of these input SQUIDs. Additional reduction in wire count is achieved by using common bias lines for multiple TES bias circuits; each bias circuit consists of a shunt resistor, the TES, the SQUID input coil, and additional inductance for filtering the detector response. Columns of

individual bias circuits are biased in series with a common dc current. The reference design is based on 32-row multiplexing, with which the entire XMS focal plane array can be instrumented with 68 signal channels. Figure 4 is a schematic of the TDM read out, Figure 5 is a photograph of the detector and readout components used in a demonstration of 2 columns of 8-row multiplexing of a GSFC TES array using the NIST multiplexer, and Figure 6 shows spectra acquired in that demonstration.

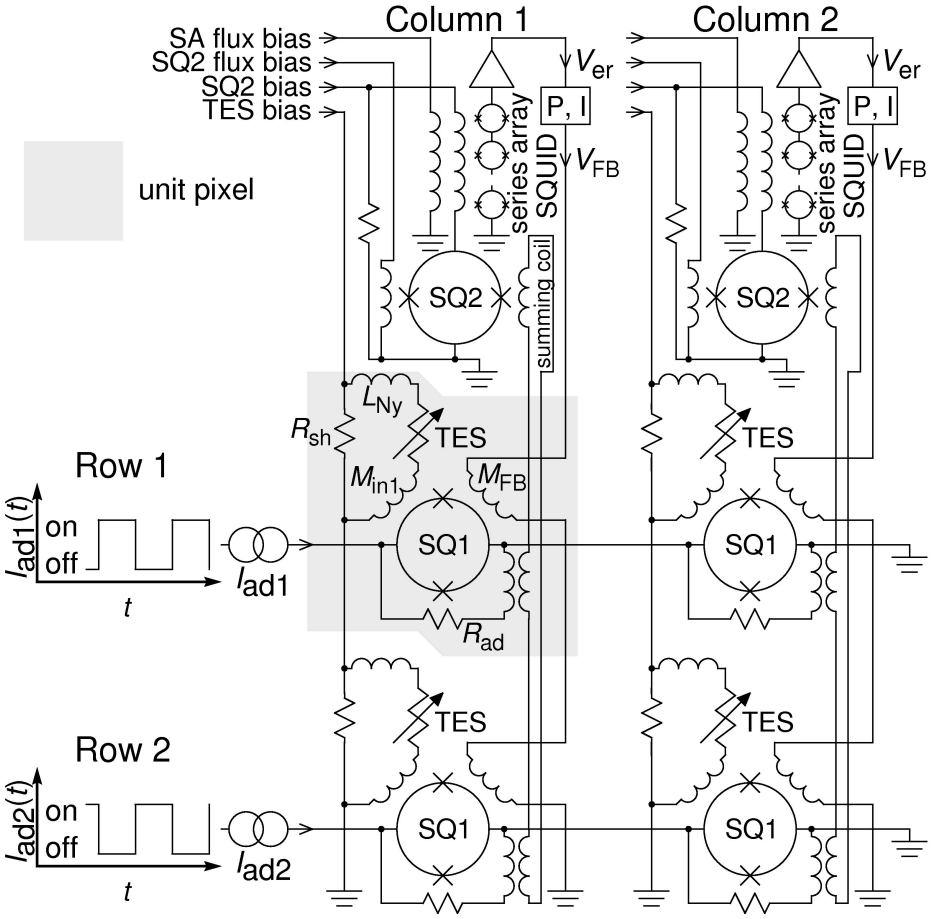


Fig. 4: Schematic of a 2-row x 2-column SQUID-time-division multiplexer, used to illustrate a general N-row x M-column array. Each TES is inductively coupled ($M_{in1}$) to its own first-stage SQUID amplifier (SQ1). The TESs are dc biased. An inductive summing coil carries the output signals from all SQ1's in a column to a common second-stage SQUID (SQ2). Rows of SQ1s are sequentially turned on (or addressed, using $I_{ad}$), so the signal from one TES at a time per column is passed to that column's SQ2. When a SQ1 is off, it is essentially a superconducting wire, transmitting no signal from its TES and no noise. Finally, the output of each SQ2 is routed to a 100-SQUID, series-array amplifier and then to room-temperature electronics. In order to keep the nonlinear three-stage SQUID amplifier in a small, linear range, the multiplexer is run as a flux-locked feedback loop. The series array output, or error signal ($V_{er}$) is digitally sampled, and then a flux-feedback signal ($V_{FB}$) is applied inductively to the first-stage SQUIDs to servo $V_{er}$ to a constant value. A linear combination of $V_{FB}$ and $V_{er}$ gives the TES current. Electronics synchronize the row-address and flux-feedback signals and stream the data to a computer. A kilopixel array could be read out with a 32-row x 32-column TDM.

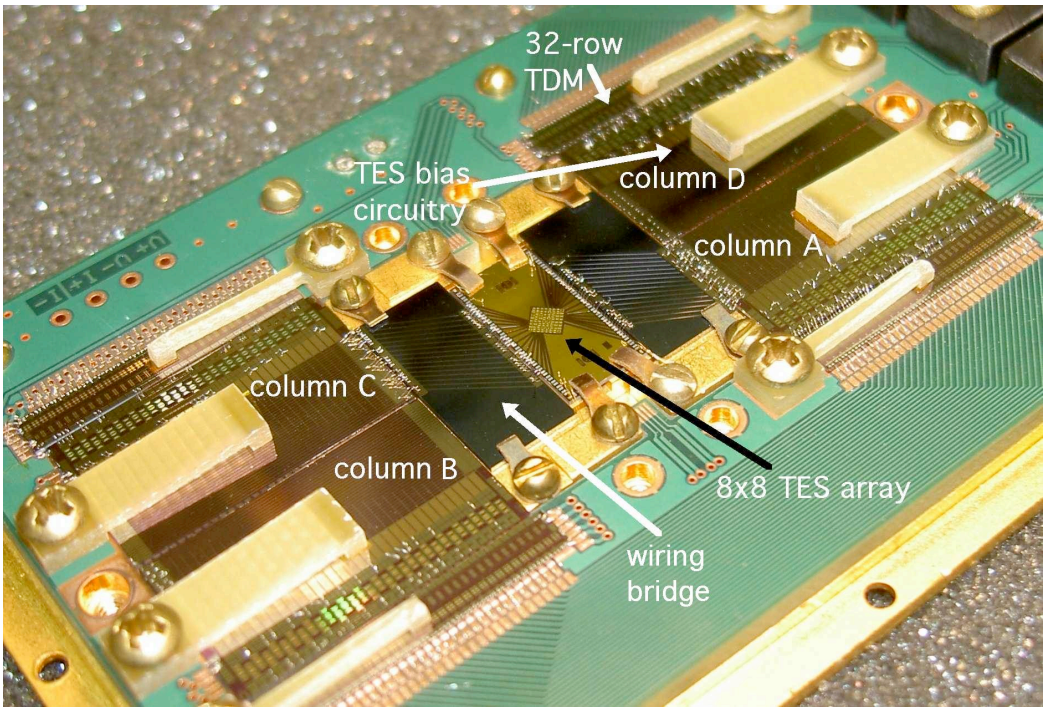


Fig. 5: Laboratory 4x32 SQUID TDM test card at NIST, with GSFC 8x8 TES array installed.

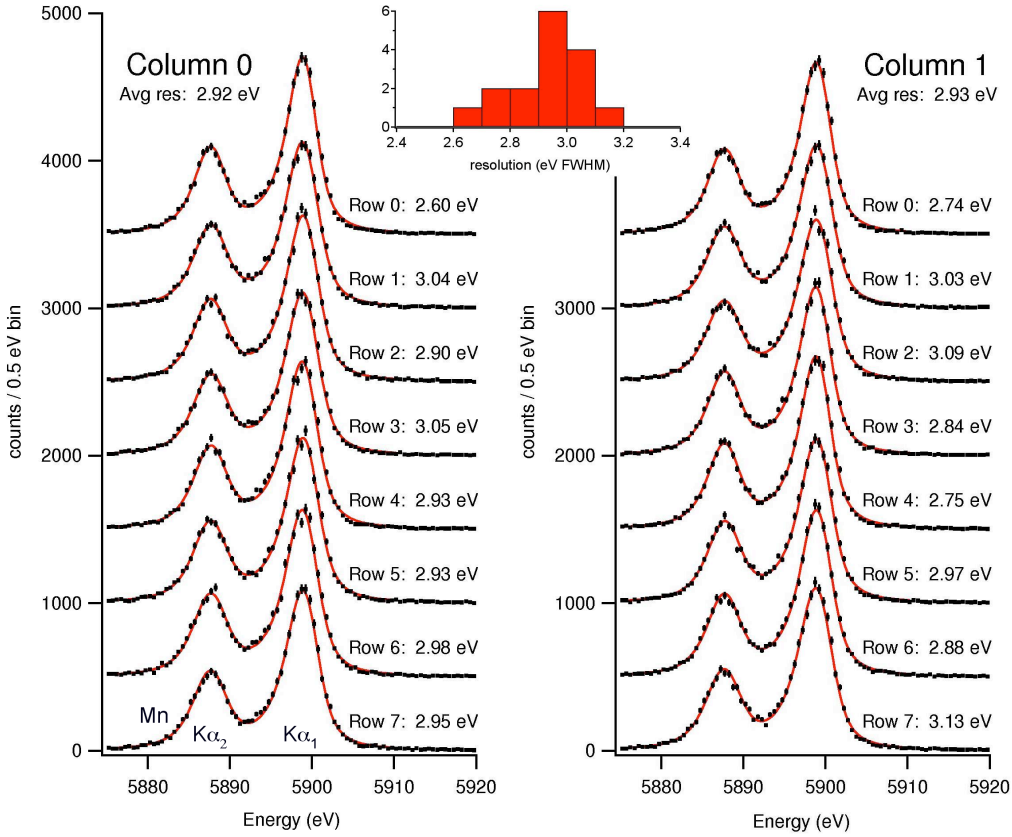


Fig. 6: Energy resolution values measured on 16 channels multiplexed in set-up of Fig. 6.

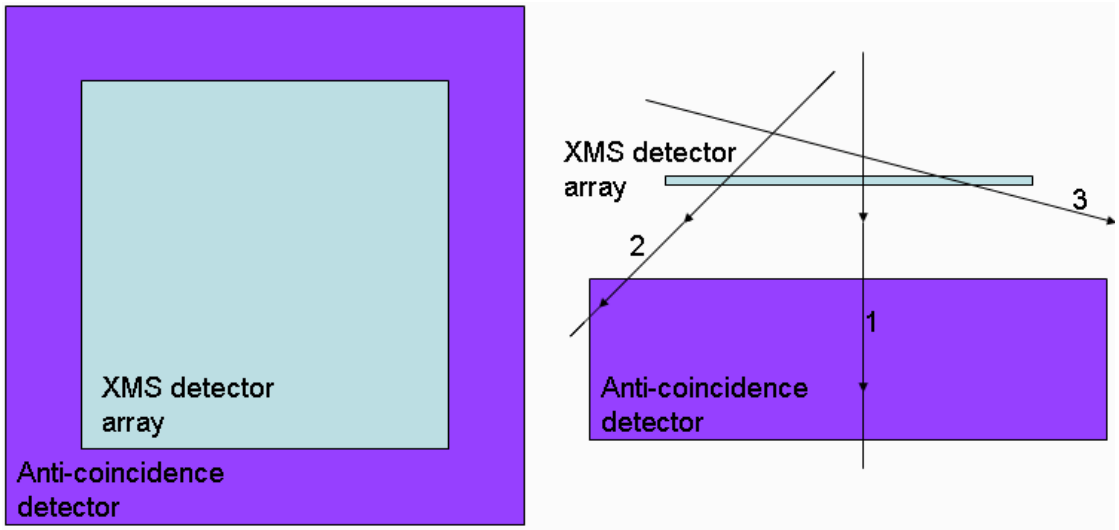


Fig. 7: Schematic showing placement of the anti-coincidence detector relative to the XMS array. LEFT: Face-on view, showing extent of the anti-coincidence device beyond the calorimeter array. RIGHT: Cross section, showing how, for minimum ionizing particles, a single-sided veto scheme is adequate. Three proton tracks are shown. Events resulting from tracks 1 and 2 are rejected by coincidence. Track 3 is rejected because it deposits enough energy over its long track in the calorimeter absorber that it is above the XMS observing band.

BACKGROUND REJECTION: The XMS design includes a particle background veto installed behind the calorimeter array. Minimum ionizing particles, which are expected to be the main source of in-band background events, deposit around 4 MeV/cm in Si. A particle traversing a 400 μm Si wafer will therefore deposit at least 160 keV. Instrumented with TES sensors to detect the non-thermal phonon signal from these events, such a wafer placed in close proximity to the microcalorimeter array serves as a fast and highly efficient anti-coincidence detector. Particle detectors based on this principle have been used in ground-based dark matter searches for years. A schematic of the positioning of the anti-coincidence detector is shown in Figure 7. A single-sided particle veto was implemented behind the Suzaku XRS calorimeter, and is planned for the Astro-H SXS. The XMS background requirement is 4x the XRS residual background. Additional particle veto planes, in order to better identify events due to secondary particles produces in the vicinity of the detectors, will be considered if Monte Carlo simulation show such would be beneficial.

COOLING SYSTEM: The calorimeter array, the particle veto, and the front-end electronics (all of the SQUID components) are operated at a temperature of 50 mK. This temperature is established by a multi-component cooling system consisting of a multi-stage adiabatic demagnetization refrigerator (ADR) heat sunk to a multi-stage mechanical cooler based on the JWST/MIRI design. In the reference design, the ADR uses five stages to provide continuous cooling to 50 mK. Three of the stages cycle in temperature as they carry heat from the coldest stage to the warmest, but one of the intermediate stages is designed to provide a fixed thermal interface at 1 K to provide a stable thermal shield and heatsink for wires. Figure 8 shows a laboratory prototype of a multi-stage continuous ADR being developed at Goddard. In the reference design, the

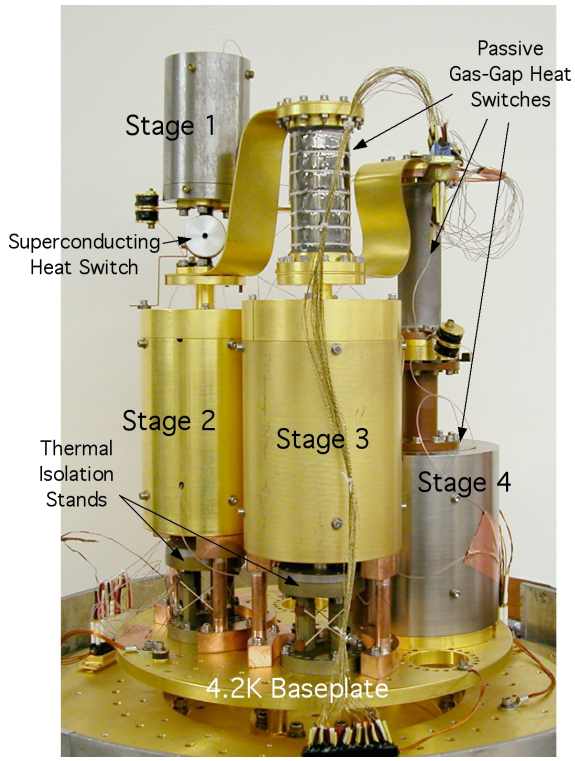


Fig. 8: GSFC prototype of a 4-stage continuous ADR.

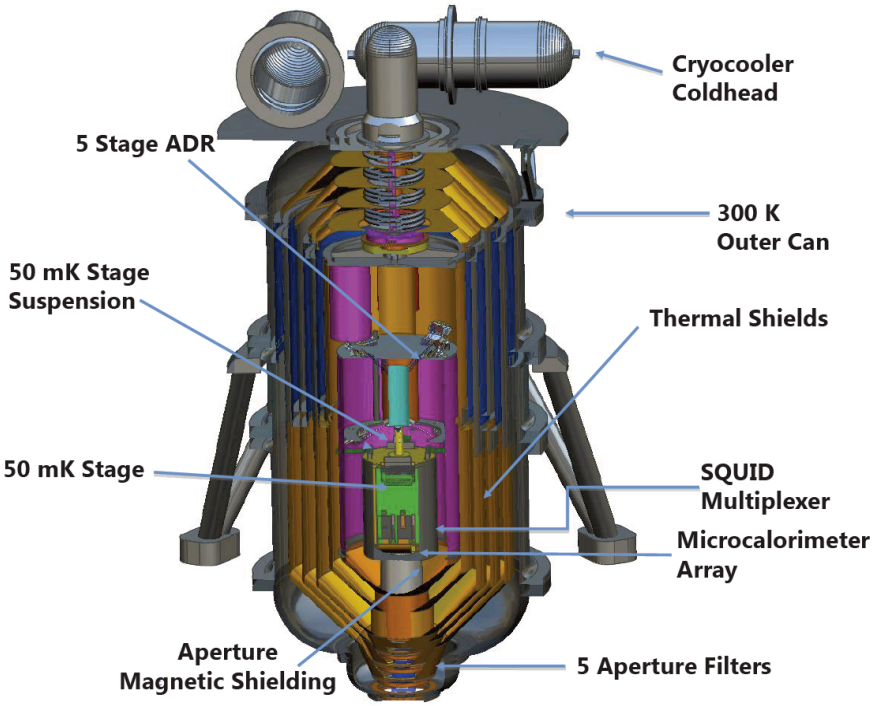


Fig. 9: Cut-away view of the XMS cryostat. The mechanical cooler interface is at the top. The focal plane and the ADR are contained in a central volume enclosed in a thermal shield cooled by the JT cooler to 4.5 K.

ADR dumps heat to a 4.5 K interface cooled by a $^4$He Joule-Thomson cooler (JT), which, in turn, is cooled by a three-stage pulse-tube cooler. This configuration for the mechanical cooler is based on JWST/MIRI. The stages of the pulse-tube cooler provide thermal interfaces at 120K, 45 K, and 15 K, and the temperature of the outer shell of the XMS dewar will be < 300 K. Interior thermal shields and cables from 50 mK are heat sunk to several intermediate temperature stages. The cooling system uses no cryogens. Figure 9 illustrates the cryostat architecture. Magnetic shielding, using both superconducting and high-permeativity metals, is used to reduce static and fluctuating magnetic fields in the vicinity of the detectors and the SQUIDs.

DETECTOR ASSEMBLY: The detector assembly houses and provides the thermal staging at 50 mK (for the TES arrays, the particle veto, and the SQUIDs), at 1 K (for heat intercepts on the wiring) and at 4.5 K (for the termination resistors used on the SQUID feedback and address lines). The 50 mK, 1 K, and 4.5 K sections are held rigidly with respect to each other so that the assembly can be inserted as a single unit with minimized thermal conduction between the stages. The assembly includes mechanical suspension systems, heat sinks, wiring interconnects, high density wiring feedthroughs, and magnetic shielding. It is designed to provide the 50 mK interface to the calorimeter and, along with the design of the array itself, establish temperature uniformity across the array adequate to meeting the resolution requirements. The design also keeps thermal and electrical crosstalk to a level compatible with the requirements. The estimated conducted and dissipative heat loads due to the detector assembly are shown in Table 1.

| Temperature stage | Conducted and dissipated heat load due to the detector assembly |
|---|---|
| 50 mK | 1 μW |
| 1 K | 4 μW |
| 4.5 K | 0.35 mW (from dissipation in the termination resistors) |

Table 1: conducted and dissipative heat loads due to the detector assembly

IR BLOCKING FILTERS AND FILTER WHEEL: The XMS requires a series of blocking filters to minimize the thermal load on the coldest stages of the dewar system and detector array, yet provide the highest possible X-ray transmission. A series of five thin aluminized polymer-film filters, each connected to a different temperature stage, will be used. These filters are mounted in a cylindrical baffle. The total filter stack consists of 280 nm of polymide and 210 nm of Al, resulting in the transmission shown in Fig. 10.

A filter wheel above the focal plane will be used to rotate different filters into the aperture. One of these will be open, and another will contain a diffuser based on microchannel-plate optics, to spread the light of bright point sources over the array. Additional positions will be used for increased optical blocking (to mitigate photon

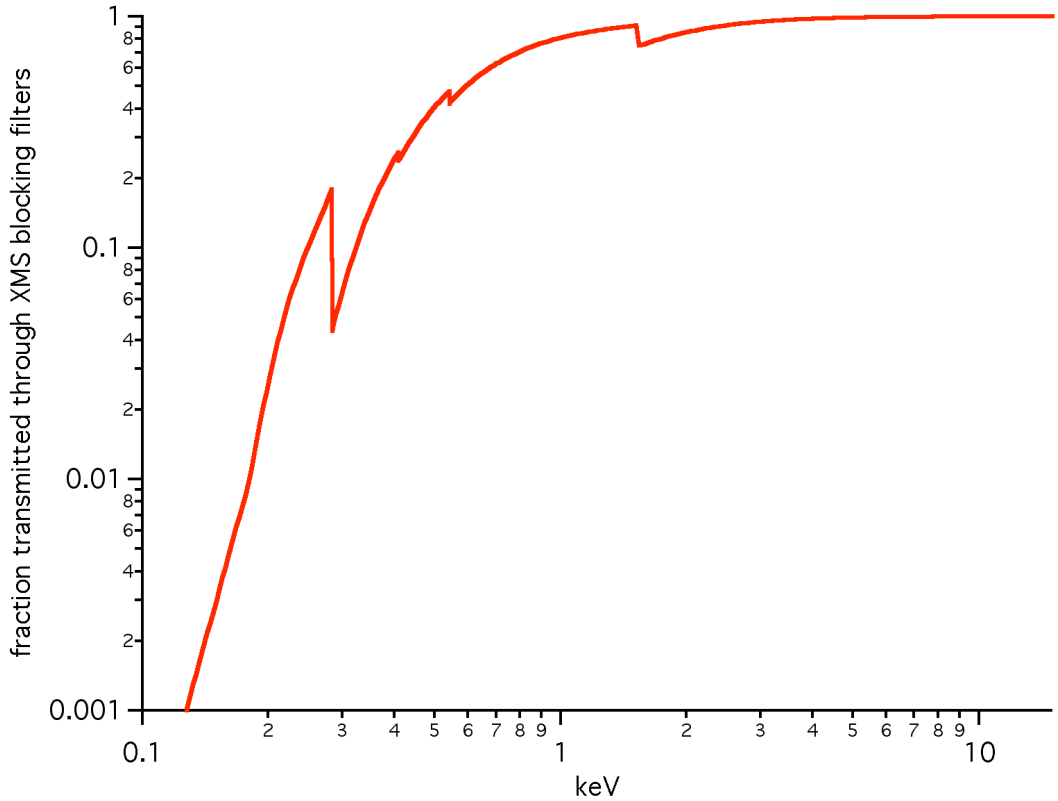


Fig. 10. Transmission of the XMS filter stack in the reference design.

noise from sources with high flux at wavelengths longer than UV) or for attenuation of soft x-rays in observations for which a high rate in the Fe-K lines is the most important. An electronically controlled x-ray source for calibration and gain monitoring will be mounted on the fixed mount of the filter wheel mechanism so that it can be operated with any filter position in place. Back-up radioactive calibration sources will be placed in positions in the filter wheel.

<u>INSTRUMENT ELECTRONICS</u>: The instrument electronics include the drive electronics for the filter wheel and the mechanical coolers, the ADR controller (including temperature control to 2 uK RMS), thermometry monitoring, multiplexer control electronics, and signal processing. Only the signal electronics involve high data rates. Power estimates for the electronics (and for the cooler itself) are tabulated in Table 3.

Figure 11 is a simplified schematic of a channel of signal electronics. Outside of the dewar, the signals pass through three types of electronics boxes – a preamplifier box located close to the dewar, a digital feedback controller that determines and switches the SQUID feedback synchronously with the row address switching, and a pulse processing unit that demultiplexes the data, triggers signal pulses, and optimally filters the signals to determine the energy of each x-ray pulse. The reference design presumes 68 channels with 32-row multiplexing per channel, with

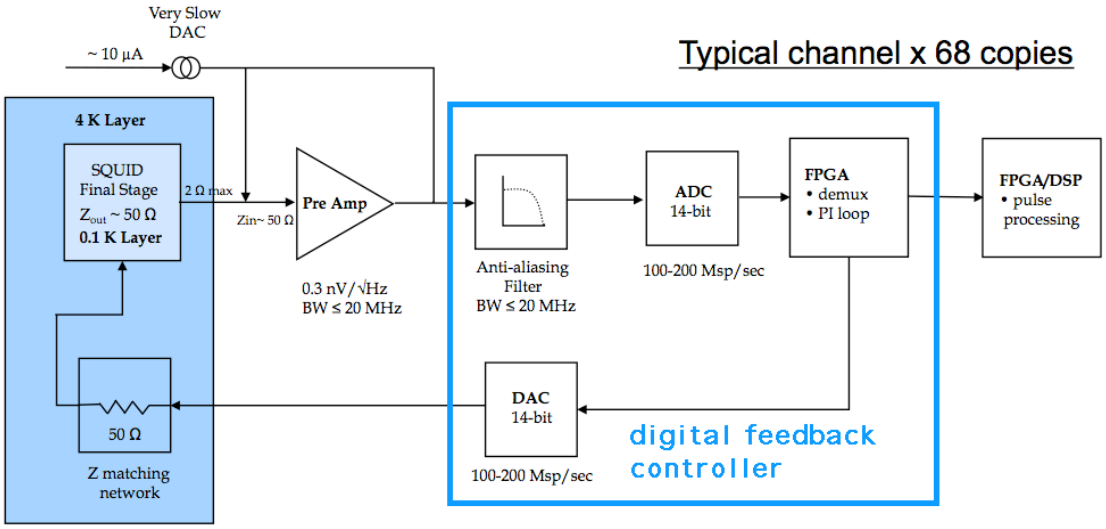


Fig. 11: Schematic of a multiplexed signal channel for the XMS reference configuration. Digital feedback is used to linearize the response of the SQUID amplifiers (see Fig. 4). Outside of the cryostat, the functions reside in 3 box types – a preamp mounted close to the dewar, a digital feedback controller box that determines and switches the SQUID feedback synchronously with the address switching, and a pulse processing unit that demultiplexes the data, triggers signal pulses, and optimally filters the signal to determine the energy.

a frame rate of 200 KS/sec. The line rate is thus 6.4 MS/sec. Several ADC samples are needed per line sample in order to sample the data after the switching transients have settled. The present architecture uses 32 samples, but this can be reduced to at least 16, and probably lower. Given 14-bit samples, the data rate going into demultiplexing is 97 Mb/s per column. This rate is constant, independent of the flux incident on the array. The reference design also assumes the anti-co has 4 single channels (one per quadrant) read out at the frame rate of the science array.

Each processed event requires 64 bits to communicate energy, pixel number, time, and various flags and diagnostic parameters. For a typical observation of 500 counts/sec over the array, the science data require 32 kb/s of telemetry. At the maximum rate required, 20,000 counts/sec, the data rate would be 1.28 Mb/s for 64-bit events, but compression of the time encoding will be possible at the high rates.

<u>OPERATIONAL MODES</u>: The XMS will use the following operational modes.

A – SCIENCE

1) <u>Nominal Science Mode</u> – Science observations in progress, everything on (mechanisms as needed)
2) <u>Calibration Mode</u> – Once daily, motion of filter wheel and/or activation of powered x-ray source
3) <u>Optimal Digital Filter Generation</u> - (as required, possibly once per month), in conjunction with calibration mode operations

B. ENGINEERING

1) Standby (temperature monitoring); cryocooler, cryocooler control electronics, and ADRs on; detector electronics on but no processing (low power mode); no mechanism movements inherent in this mode

2) Diagnostic (I-V curves, V-Φ curves, etc), consumes full power as nominal science

3) Power Save (i.e., not in Field of View), cryocooler, cryocooler control electronics on; ADR off; detector and all other electronics off; no mechanism movements inherent in this mode

4) Cool Down – Post Launch/Safemode Checkout, power on cryocooler, cryocooler control electronics, and ADRs; thermal stabilization; detector electronics on but no processing (low power mode); mechanism movements possible

C - SAFE MODE

1) Initial Safemode – Spacecraft activates, same as Standby

2) Deep Safemode - Spacecraft activates, same as Power Save (further loadshedding)

3) Critical Safemode - Spacecraft activates, XMS entirely off to ensure power positive spacecraft

D - OFF

REQUIREMENTS AND INSTRUMENT ACCOMMODATIONS: Requirements, mass, and power are summarized in the following tables. The requirements are independent of implementation, but mass and power are based on the specific reference design described in this document.

*Table 2: Instrument scientific requirements*

| Parameter | Requirement | Comment |
|---|---|---|
| **Inner array** | | |
| Energy range | 0.3 – 10 keV | Goal: 0.1 – 12 keV |
| Energy resolution (E < 6 keV) | 2.5 eV | |
| FoV | 2 arcmin | Corresponds to 40 x 40 pixels |
| Pixel size | 300 μm | The PSF (5 arcsec) corresponds to 0.5 mm and as such the pixel size is a compromise between FoV and undersampling of the PSF |
| Signal decay time (1/e) | 300 μs | Goal: 200 μs |
| **Outer array** | | |
| Energy range | 0.3 – 10 keV | Goal: 0.1 – 12 keV |
| Energy resolution (E < 6 keV) | 10 eV | |
| FoV | 5.4 arcmin | Corresponds to a detector size of 31.2 x 31.2 $mm^2$ |
| Pixel size | 600 μm | 4 pixels will be read-out by a single TES with different thermal conductance between each pixel and the TES |
| Signal decay time (1/e) | 2000 μs | Due to larger pixel size |
| **Full array** | | |
| Absolute Time | 50 μs | Similar to HTRS |
| Time resolution | 10 μs | |
| Maximum count rate input on instrument | 120.000 cnts/sec | Observation of the Crab (120,000 cts/s) will be feasible using a diffuser (reduction > 0.15) |
| Maximum output from the instrument | 20.000 cnts/sec | Capability of backend processing for full detector array. At these rates the energy resolution could degrade (see requirement on the good grade events) |
| Typical count rate | 500 cnts/sec | During a typical observation (4 mCrab) |
| good grade events | 50 counts/sec/pixel | >80% of the events will provide the nominal energy resolution. For bright point sources with > 100 cts/s/pixel a diffuser can be included in the beam. This will introduce a reduction in the effective area. |
| Event size | 42 – 64 bits | Depends on the user defined accuracy, spacecraft should be able to handle 64 bits/event |
| Quantum efficiency @ 1 keV | > 60 % | Entire instrument efficiency (e.g. blocking support structure in filters result in a QE ~ 0.7 and packing efficiency (~ 95%) |
| Quantum efficiency @ 7 keV | > 80 % | Defines absorber thickness |

| | | |
|---|---|---|
| Energy resolution uniformity (FWHM) | 1 eV | Fit by a Gaussian distribution |
| Detector dead area | < 5% | Pixels with E-resolution > 3 * nominal or QE < 0.5 nominal QE |
| Straylight at main shell filter<br>at 0.5 μm<br>at 10 μm | <br>< 2.5 $10^9$ ph/cm$^2$/s<br>< $10^{17}$ ph/cm$^2$/s | Straylight will degrade the energy resolution of the detector. The specified levels are indicative and correspond to a degradation of the spectral resolution of less than 1 eV.. |
| Micrometeorites | < 38 pinholes of 100 μm diameter in OBF | Corresponds to a degradation of the energy resolution of 0.2 eV |
| Effective area change due to contamination over lifetime | < 10 % over 0.2 < E < 1 keV | Depending on the contaminant (water) or hydrocarbons |
| Transmission fixed optical filters<br>at 0.25 keV<br>at 1.0 keV<br>at 6 keV | <br>0.1<br>0.7<br>0.9 | Corresponds to 5 filters similar to those planned for Astro-H. The goal is to Si mesh filters with 20 nm Al and 45 nm parylene, increasing the transmission at low energy by a factor 2 |
| Non X-ray background | 2 $10^{-2}$ counts/cm$^2$/keV/s | This number is 4 times the background measured in Suzaku (due to the different orbit). In narrow lines this contribution is negligible. This level requires an anti-coincidence detector |
| Continuous observing time | > 31 hour | Dimensions the cooling system |
| Instrument setup time | 1 hour | 1 hour to stabilize the instrument response such that, after corrections, the nominal resolution is achievable |
| Regeneration time | < 10 hr | Could be considerably shorter (1 hr) |
| Energy scale stability | 1 eV / h | The non-correctable drifts are part of the energy resolution. Drifts in the order of 1eV/h can be corrected. This requires:<br>- a stable environment of the electronics<br>- the capability to monitor the energy scale using onboard calibration sources (either on the filter wheel or electronically controlled) |
| Relative uncertainty in QE between pixels | < 3 % | This will be achieved by a combination of measures:<br>- ground calibration<br>- in-orbit verification on chosen sources<br>- on-board calibration sources<br>- dithering (to disentangle QE variations from source variations |

*Table 3: Mass and Power for US reference design*

| Item | Quantity | Mass | Power (W) | | |
|---|---|---|---|---|---|
| | Flight Set | CBE Total Flght Mass (kg) | Science Average | Safehold | Peak |
| **XMS MASTER EQUIPMENT LIST** | | | | | |
| **INSTRUMENT TOTAL** | | **263** | **649** | **0** | **1385** |
| XMS | 1 | 262.9 | 649 | 0 | 1385 |
| Filter Wheel Mechanism | 1 | 6.8 | | | |
| Gate Valve | 1 | 0.0 | | | |
| Pyro Devices for Gate Valve | 1 | 0.2 | | | |
| XMS Cryostat Assembly | 1 | 86.7 | | | |
| Dewar Bipod Assembly | 3 | 9.0 | | | |
| XMS Electronics Boxes | 1 | 109.3 | 434 | 0 | 600 |
| XMS Thermal Subsystem | 1 | 19.0 | 0.0 | 0 | 570 |
| Cryocooler | 1 | 31.9 | 215 | 0 | 215 |